EFFECTIVE FIELD THEORY FOR ROTATIONAL BANDS IN DEFORMED AND SUPERDEFORMED NUCLEI*

P. Ring

Physikdepartment der Technischen Universität München
85748 Garching, Germany

and A.V. Afanasjev†

Physics Division, Argonne National Laboratory
Argonne, IL 60439, USA

(Received August 10, 2001)

An overview is given on the description of rotational bands in normally deformed and superdeformed nuclei in the framework of effective field theories such as the Relativistic Mean Field (RMF) theory and the Relativistic Hartree–Bogoliubov (RHB) theory. In particular we discuss recent investigations for the description of superdeformed bands in the $A \sim 60$, 140–150 and 190 mass regions and compare them briefly with the results obtained in non-relativistic mean field theories.

PACS numbers: 21.60.Cs, 21.60.Jz, 27.80.+w

1. Introduction

In recent years is has become very popular to describe the structure of nuclei in the framework of relativistic field theories based on effective Lagrangians. Relativistic Mean Field (RMF) theory *i.e.* the extension of the Walecka model to non-linear meson couplings is one of the most prominent examples. It is conceptually similar to density dependent Hartree-Fock theory with Skyrme forces, which is nowadays standard for the microscopic

* Invited talk presented at the *High Spin Physics 2001* NATO Advanced Research Workshop, dedicated to the memory of Zdzisław Szymański, Warsaw, Poland, February 6–10, 2001.

† On leave of absence from the Laboratory of Radiation Physics, Institute of Solid State Physics, University of Latvia, 2169 Salaspils, Miera str. 31, Latvia.

description of nuclear properties over the entire periodic table. It shares with this theory, that it contains only a few parameters which are adjusted to data of nuclear matter and a few closed shell nuclei. All the other nuclei are described with one parameter set. In contrast to the non-relativistic density functional theories it has the advantage, that it fully incorporates relativity. This leads to large attractive scalar and large repulsive vector fields, which cancel to a large extent in the normal nuclear potential leading to relatively small Fermi momenta and non-relativistic kinematics. However they add up in the potentials for the small components leading to a large spin-orbit splitting and to pseudospin-symmetry. In this way covariant density functional theories incorporate essential effects in a fully self-consistent way with a small number of parameters.

In this contribution we summarize a number of investigations within the relativistic framework devoted to rotating nuclei, in particular those with superdeformed shapes.

2. Relativistic Mean Field theory in rotating frame

RMF theory describes the nucleus as a system of nucleons (Dirac spinors) which interact in a relativistic covariant manner through the exchange of virtual mesons [1]: the isoscalar scalar σ meson responsible for the large scalar attraction at intermediate distances, the isoscalar vector ω meson responsible for the vector repulsion at short distances and the isovector vector ρ meson which takes care for the asymmetry properties of nuclei with large neutron or proton excess. In addition, the photon field (A) accounts for the electromagnetic interaction.

RMF theory has been extended for the description of rotating nuclei to cranked relativistic mean field (CRMF) theory by employing the cranking idea in Refs. [2–4]. In the first applications pairing correlations were neglected and cranking was performed for a fixed axis perpendicular to the symmetry axis. The CRMF equations include the Dirac equation in the Hartree-approximation for fermions

$$\Big\{\boldsymbol{\alpha}(-i\boldsymbol{\nabla} - \boldsymbol{V}(\boldsymbol{r})) \;+\; V_0(\boldsymbol{r}) \;+\; \beta(m + S(\boldsymbol{r})) - \Omega_x \hat{J}_x\Big\}\psi_i \;=\; \varepsilon_i \psi_i\,, \quad (1)$$

where $V_0(\mathbf{r})$ represents a repulsive vector potential, $S(\mathbf{r})$ an attractive scalar potential, $\boldsymbol{V}(\boldsymbol{r})$ the magnetic potential, and the term $\Omega_x \hat{J}_x$ the Coriolis field. The time-independent inhomogeneous Klein–Gordon equations for mesonic fields are given by

$$\begin{aligned}
\left\{-\Delta - (\Omega_x \hat{L}_x)^2 + m_\sigma^2\right\}\ \sigma(\boldsymbol{r}) &= -g_\sigma \rho_s(\boldsymbol{r}) - g_2\sigma^2(\boldsymbol{r}) - g_3\sigma^3(\boldsymbol{r})\,, \\
\left\{-\Delta - (\Omega_x \hat{L}_x)^2 + m_\omega^2\right\}\omega_0(\boldsymbol{r}) &= g_\omega \rho_v(\boldsymbol{r})\,, \\
\left\{-\Delta - (\Omega_x (\hat{L}_x + \hat{S}_x))^2 + m_\omega^2\right\}\ \boldsymbol{\omega}(\boldsymbol{r}) &= g_\omega \boldsymbol{j}(\boldsymbol{r})\,,
\end{aligned} \tag{2}$$

with source terms involving the various nucleonic densities and currents calculated by summing over the levels in the Fermi sea only (*no-sea approximation*). For simplicity, the equations for the ρ meson and the Coulomb fields are omitted in Eqs. (2) since they have the structure similar to the equations for the ω meson.

CRMF theory has been used extensively in the study of SD bands in which the pairing correlations are expected to play only a minor role. This approach has an advantage since the question of a self-consistent description of pairing correlations in finite nuclei starting from a relativistic Lagrangian still remains a not fully solved theoretical problem [5]. Considering, however, that the pairing is a genuine non-relativistic effect, which plays a role only in the vicinity of the Fermi surface one can consider the pairing correlations only between the baryons using the pairing part of the phenomenological Gogny interaction with finite range in the particle-particle (pairing) channel. In conjunction with RMF theory such an approach to the description of pairing correlations has been applied, for example, in the study of ground state properties, neutron halos and deformed proton emitters. Recently Cranked Relativistic Hartree–Bogoliubov (CRHB) theory has been applied for super-deformed bands in the Hg-region.

The CRHB equations for the fermions in the rotating frame are given in one-dimensional cranking approximation by

$$\begin{pmatrix} h - \Omega_x \hat{J}_x & \hat{\Delta} \\ -\hat{\Delta}^* & -h^* + \Omega_x \hat{J}_x^* \end{pmatrix} \begin{pmatrix} U_k \\ V_k \end{pmatrix} = E_k \begin{pmatrix} U_k \\ V_k \end{pmatrix}\,, \tag{3}$$

where $h = h_{\mathrm{D}} - \lambda$ is the single-nucleon Dirac Hamiltonian minus the chemical potential λ and $\hat{\Delta}$ is the pairing potential. U_k and V_k are quasi-particle Dirac spinors and E_k denote the quasi-particle energies. An additional feature is that in CRHB theory we go beyond the mean field and perform an approximate particle number projection before the variation by means of the Lipkin–Nogami method [6–8]. It turns out that this feature is extremely important for a proper description of the moments of inertia.

The spatial components of the vector mesons give origin to a magnetic potential $\boldsymbol{V}(\boldsymbol{r})$ which breaks time-reversal symmetry and removes the degeneracy between nucleonic states related via this symmetry [4, 9]. This

effect is commonly referred as *nuclear magnetism* [2]. It is very important for a proper description of the moments of inertia [4]. Consequently, the spatial components of the vector ω and ρ mesons are properly taken into account in a fully self-consistent way in the calculations.

The microscopic relativistic and non-relativistic mean field approaches being fully self-consistent share some common features, for example, such as the low effective mass being typically in the range of 0.6–0.7 and the presence of time-odd mean fields which have a large impact on the moments of inertia. The low values of the effective mass in microscopic theories lead to a low level density in the vicinity of the Fermi level compared with experiment. This problem can, in general, be cured by taking into account the coupling between single-particle motion and low-lying collective vibrations. The time-odd mean fields, which play an important role in rotating nuclei, are defined uniquely in the RMF theory, while in the approaches based on effective interaction of Skyrme type this depends on underlying energy functional or the corresponding effective two-body interaction. A clear advantage of RMF theory is the fact that the spin-orbit term emerges in a natural way, while it has to be parametrized in the non-relativistic approaches. RMF theory is distinct from non-relativistic theories in the mechanism of nuclear saturation, where the nucleonic potential emerges as a difference of large attractive scalar ($S(\boldsymbol{r})$) and repulsive vector ($V_0(\boldsymbol{r})$) potentials.

Theoretical approaches, based on the non-relativistic macroscopic + microscopic method, which use the Woods–Saxon or Nilsson potentials for the microscopic part still remain very powerful tools for our understanding of rotating nuclei. By treating the bulk and the single-particle properties separately they have the advantage to fit many details of the actual nuclei directly to the appropriate region under investigation. However, this separation leaves some room for inconsistencies between the macroscopic and microscopic parts. In addition, time-odd mean fields are neglected in this method. However, these phenomenological models have some advantages related to the facts that *(i)* the effective mass is one by definition, *(ii)* they are more flexible due to the separation of bulk and single-particle properties, *(iii)* the numerical calculations are by orders of magnitude less time consuming than the ones in the microscopic approaches.

3. Superdeformation in the regime of weak pairing correlations

CRMF theory has been extensively used for the description of SD bands in which the pairing correlations are expected to be considerably quenched. Detailed investigations have been performed using this approach in the $A \sim 140$–150 and in the $A \sim 60$ mass regions. One should clearly recognize that the neglect of pairing correlations is an approximation because pairing

correlations being weak are still present even at the highest rotational frequencies. However, the question of the description of pairing correlations in the regime of weak pairing still remains an open problem (see, for example, the introduction in Ref. [9]). Almost all cranked mean field approaches which aim to describe pairing correlations in rotating nuclei use an approximate particle number projection before variation by means of the Lipkin–Nogami method. However, the applicability of this method in the regime of weak pairing correlations as an approximation to exact particle number projection seems questionable. Keeping this in mind we think that the neglect of pairing correlations is a reasonable approximation in a specific physical situations and, although some specific features such as, for example, paired band crossings cannot be addressed, it allows to gain considerable understanding of physical phenomena in the high spin region.

3.1. The $A \sim 140$–150 mass region

Since the discovery of superdeformation in ^{152}Dy in 1986 this mass region was the testing field for different theoretical models and concepts. Already the investigations within the macroscopic + microscopic method gave an understanding of the impact of different single-particle orbitals on the dynamic moments of inertia $J^{(2)}$ and transition quadrupole moments Q_t, possible underlying mechanisms of identical bands, methods of configuration assignment based on properties of dynamic moments of inertia or effective alignments $i_{\rm eff}$ and so on. These developments are covered in review articles [10, 11].

A systematic investigation of the properties of the SD bands in this mass region has been performed in the framework of the CRMF theory [9,17]. It was shown that CRMF theory reproduces well the experimentally observed features such as the properties of dynamic moments of inertia $J^{(2)}$, single-particle ordering in the SD minimum, alignment properties of single-particle orbitals etc. Calculated charge quadrupole moments Q_0 are in general somewhat larger than the average experimental values quoted in literature but they are still within the experimental error bars if the uncertainties due to stopping powers ($\sim 15\%$) are taken into account. The last feature is also typical for other theoretical approaches based either on the Nilsson or the Woods–Saxon potentials and Skyrme forces.

3.2. The $A \sim 60$–70 mass region

As illustrated in Fig. 1, the rotational properties of the SD band in ^{60}Zn are distinctly different from the ones seen in the $A \sim 150$ and 190 mass regions. Indeed, at the highest rotational frequencies the dynamic moment of inertia $J^{(2)}$ is only approximately 60% of the kinematic moment of inertia $J^{(1)}$. The comparative study of SD and highly deformed bands

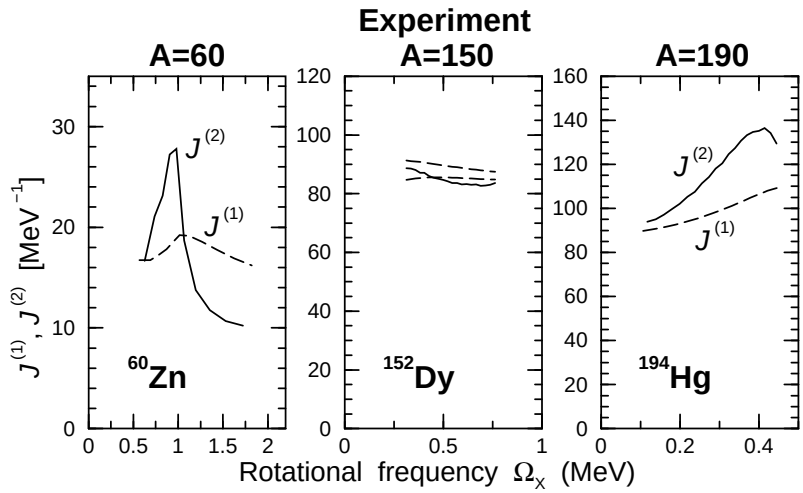

Fig. 1. Dynamic ($J^{(2)}$) and kinematic ($J^{(1)}$) moments of inertia of representative SD bands observed in the $A \sim 60$, 150 and 190 mass regions. SD bands in ^{60}Zn and ^{194}Hg are linked to the low-spin level scheme. On the contrary, no SD band in $A \sim 140$–150 mass region is linked to the low-spin level scheme. Thus the $J^{(1)}$ values for the SD band in ^{152}Dy are shown under two different spin assignments: the lowest transition in SD band with energy 602.4 keV corresponds to the spin changes of $26^+ \to 24^+$ (lowest curve) and of $28^+ \to 26^+$ (highest curve).

in this mass region has been performed within the framework of the CRMF theory and CNS approach based on the Nilsson potential in Refs. [12–14]. Defining the spin values of the unlinked SD and highly deformed bands by means of effective alignment approach it was shown that also other bands of these types show the same relation between $J^{(1)}$ and $J^{(2)}$, see Fig. 2. These features are very similar to the ones seen in smooth unfavoured terminating bands observed in the $A \sim 110$ mass region.

It turns out that the rotational properties ($J^{(1)}$ and $J^{(2)}$)[1], effective alignments $i_{\rm eff}$ and transition quadrupole moments Q_t of highly deformed and SD bands are described rather well both in the CRMF and in the CNS approaches, see Refs. [12–14] and Fig. 2 in the present manuscript, with the results of CRMF calculations being in average in better agreement with experimental data.

[1] The description of the paired band crossing observed in ^{60}Zn band at $\Omega_x \sim 1.0$ MeV is not addressed in the present calculations without pairing.

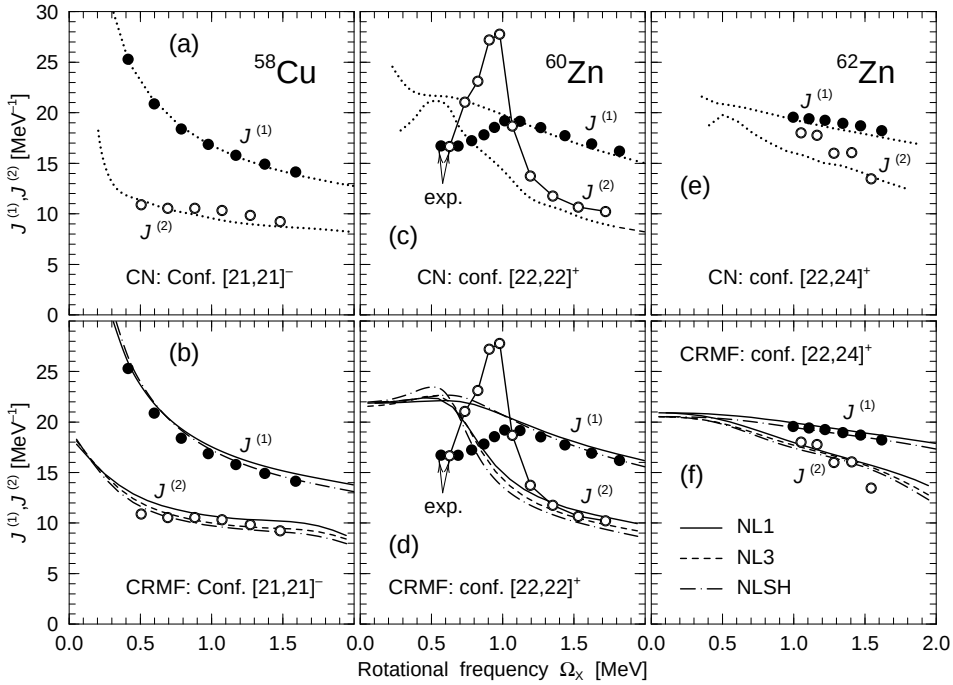

Fig. 2. Kinematic $J^{(1)}$ (unlinked solid circles) and dynamic $J^{(2)}$ (open circles) moments of inertia of observed bands versus the ones of assigned calculated configurations. The notation of the lines is given in the figure. To label the configurations we use the shorthand notation $[p_1p_2, n_1n_2]$ where p_1 (n_1) is the number of proton (neutron) $f_{7/2}$ holes and p_2 (n_2) is the number of proton (neutron) $g_{9/2}$ particles. Superscripts to the configuration labels (*e.g.* $[22,22]^{+}$) are used to indicate the sign of the signature r for that configuration ($r = \pm 1$). The values of $J^{(1)}$ calculated with NL3 are typically in between the ones obtained with NL1 and NLSH, so for simplicity they are not shown. (From Ref. [12]).

4. Superdeformation in the $A \sim 190$ mass region

The SD bands in this mass region are in most cases characterised by the dynamic moment of inertia $J^{(2)}$ which increases with increasing rotational frequency. Kinematic moments of inertia $J^{(1)}$ of linked SD bands in ^{192,194}Pb and ^{194}Hg (see Fig. 3) show the same features and in addition the relation $J^{(2)} \geq J^{(1)}$ holds. This indicates that the pairing correlations play a more important role in these bands compared with the ones observed in the $A \sim 60$ and 150 mass regions, see Sect. 3.

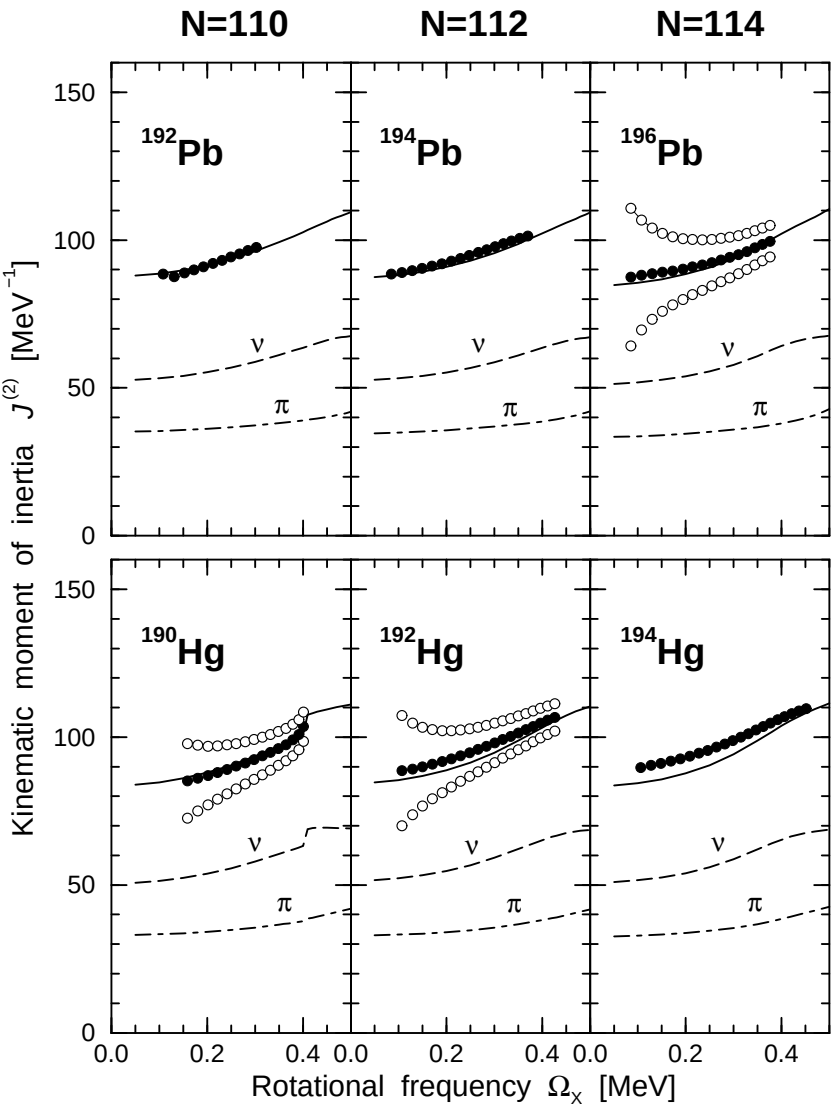

Fig. 3. Kinematic moments of inertia $J^{(1)}$. Only in the cases of the yrast SD bands in ^{192,194}Pb and ^{194}Hg, the spins of the bands are firmly (^{194}Hg, ^{194}Pb) or tentatively (^{192}Pb) defined in experiment. In other cases, the 'experimental' kinematic moments of inertia $J^{(1)}$ are shown for three different spin values of the lowest state I_0 in SD band, which are consistent with the signature of lowest calculated SD configuration. The $J^{(1)}$ values obtained in such a way are shown by circles with values being in best agreement with calculations indicated by solid circles.

Different non-relativistic approaches have been employed for the study of the superdeformation in this mass region. The CHFB calculations of SD bands in this mass region have been performed using the Gogny forces without and with approximate particle number projection before variation by means of Lipkin–Nogami method. A clear advantage of the microscopic theories based on the effective forces of the Gogny type is that no additional parameters are needed to describe the pairing correlations.

On the other hand, theoretical approaches discussed below use some assumptions about the type of pairing interaction and fit its parameters to the experimental data. An extensive investigation of SD bands in this mass region has been performed within the CHFB approach with effective forces of the Skyrme. It was concluded that special attention should be taken to the effective interaction in the pairing channel and that surface active delta pairing gives a better agreement with data for the behaviour of the dynamic moment of inertia $J^{(2)}$ versus rotational frequency than either the volume active or the seniority pairing [15].

CRHB theory has been applied to the description of the SD bands observed in even–even nuclei [16,18]. The results of the calculations for the kinematic moments of inertia are shown in Fig. 3. One can see that a very successful description of rotational features of experimental bands is obtained in the calculations without adjustable parameters. A comparison with results of other approaches based on the mean field concept indicates that the CRHB calculations provide one of best agreements with experimental data. The calculated values of transition quadrupole moments Q_t are also close to the measured ones, however, more accurate and consistent experimental data on Q_t is needed in order to make detailed comparisons between experiment and theory, for details see the discussion in Ref. [16]. RMF theory also excellently reproduces the excitation energies of the SD bands relative to the ground state in ^{194}Hg and ^{194}Pb nuclei.

The increase of kinematic and dynamic moments of inertia in this mass region can be understood in the framework of CRHB theory as emerging predominantly from a combination of three effects: the gradual alignment of a pair of $j_{15/2}$ neutrons, the alignment of a pair of $i_{13/2}$ protons at a somewhat higher frequency, and decreasing pairing correlations with increasing rotational frequency. The dynamic moments of inertia are well reproduced in the CRHB calculations [16,18]. It is also of interest to mention that the sharp increase in $J^{(2)}$ of the yrast SD band in ^{190}Hg is also reproduced in the present calculations. One should note that the CRHB calculations slightly overestimate the magnitude of $J^{(2)}$ at the highest observed frequencies. The possible reasons could be the deficiencies either of the Lipkin–Nogami method or the cranking model in the band crossing region or both of them.

5. Conclusions

The applications of the cranked versions of the relativistic mean field theory to the description of superdeformed bands in different mass regions clearly indicates that this theory provides very good agreement with experimental data. The level of agreement is comparable and in many cases better than the one obtained in the non-relativistic approaches. This is not trivial, because it is well known that the small effective mass in relativistic theories causes a considerable reduction of the level density at the Fermi surface. In a simple Inglis formula this would lead to rather large values for the moments of inertia. However, CRMF calculations are fully self-consistent, *i.e.* the inertia parameters include polarization effects and polarization currents which take into account in an average way the coupling to surface vibrations.

We would like to express our gratitude to our collaborators, who contributed to the investigations presented here, namely, to J. König, and G.A. Lalazissis. This work is also supported in part by the Bundesministerium für Bildung und Forschung under the project 06 TM 979.

REFERENCES

[1] B.D. Serot, J.D. Walecka, *Adv. Nucl. Phys.* **16**, 1 (1986).
[2] W. Koepf, P. Ring, *Nucl. Phys.* **A493**, 61 (1989).
[3] W. Koepf, P. Ring, *Nucl. Phys.* **A511**, 279 (1990).
[4] J. König, P. Ring, *Phys. Rev. Lett.* **71**, 3079 (1993).
[5] H. Kurcharek, P. Ring, *Z. Phys.* **A339**, 23 (1991).
[6] H.J. Lipkin, *Ann. Phys.* **31**, 525 (1960).
[7] Y. Nogami, *Phys. Rev.* **134**, 313 (1964).
[8] H.C. Pradhan, Y. Nogami, J. Law, *Nucl. Phys.* **A201**, 357 (1973).
[9] A.V. Afanasjev, J. König, P. Ring, *Nucl. Phys.* **A608**, 107 (1996).
[10] S. Åberg, H. Flocard, W. Nazarewicz, *Ann. Rev. Nucl. Part. Sci.* **40**, 439 (1990).
[11] C. Baktash, B. Haas, W. Nazarewicz, *Ann. Rev. Nucl. Part. Sci.* **45**, 485 (1995).
[12] A.V. Afanasjev, I. Ragnarsson, P. Ring, *Phys. Rev.* **C59**, 3166 (1999).
[13] C.E. Svensson *et al.*, *Phys. Rev. Lett.* **82**, 3400 (1999).
[14] M. Devlin, *et al.*, *Phys. Rev. Lett.* **82**, 5217 (1996).
[15] J. Terasaki, P.-H. Heenen, P. Bonche, J. Dobaczewski, H. Flocard, *Nucl. Phys.* **A593**, 1 (1995).
[16] A.V. Afanasjev, J. König, P. Ring, *Phys. Rev.* **C60**, 051303(R) (1999).
[17] A.V. Afanasjev, G.A. Lalazissis, P. Ring, *Nucl. Phys.* **A634**, 395 (1998).
[18] A.V. Afanasjev, P. Ring, J. König, *Nucl. Phys.* **A676**, 196 (2000).